A Nonlinear Observer for Integration of GPS and INS Attitude

Bjørnar Vik and Thor I. Fossen

Department of Engineering Cybernetics,
Norwegian University of Science and Technology

BIOGRAPHIES

Bjørnar Vik received his MSc degreee in Engineering Cybernetics from the Norwegian University of Technology and Science in 1994, and is currently pursuing his Ph.D. at the same university. His research interests include GPS and INS technology, nonlinear control theory especially within marine applications.

Thor I. Fossen received the M.Sc. degree in Naval Architecture in 1987 from the Norwegian University of Science and Technology (NTNU), Trondheim and the Ph.D. degree in Engineering Cybernetics from NTNU in 1991. In the period 1989-1990 Fossen pursued postgraduate studies as a Fulbright scholar in flight control at the Department of Aeronautics and Astronautics, University of Washington, Seattle. In May 1993 Fossen was appointed as a Professor in Guidance, Navigation and Control at NTNU where he is teaching ship and ROV control systems design, flight control, and nonlinear and adaptive control theory. Fossen is a Senior Scientific Advisor for ABB Industri AS, Marine Division in Oslo where he has worked on ship control. Fossen is the designer of the SeaLaunch trim and heel correction systems which is an offshore rig build by Boeing-Energia-Kværner from which rockets can be launched. Fossen is the author of the book Guidance and Control of Ocean Vehicles (Wiley, 1994) and the coeditor of the book New Directions in Nonlinear Observer Design (Springer-Verlag London, 1999).

ABSTRACT

The dynamics that describe rotation between two reference frames are in general nonlinear. Consequently, most, if not all, approaches to integration of INS and GPS attitude use an Extended Kalman filter (EKF) to perform the integration. The EKF performs well in most practical applications, but it is an approximate filter and divergence may occur from that reason. This paper presents an observer which has been designed using a nonlinear control theoretic approach. GPS measurements are used to estimate gyro biases, scale factor errors and misalignments. When the estimation errors are small, the observer becomes in effect a Luenberger observer. In this case, if Kalman filter gains are used, minimum variance estimates will be obtained. The observer has been proven to be exponentially convergent, that is, the convergence properties are essentially the same as for a linear system. Robust stability in the presence of noise and any other bounded disturbances has also been shown.
The observer has been compared to the EKF using actual GPS and IMU attitude data from a marine application, and the two show similar performance.

1 INTRODUCTION

The Extended Kalman filter (see e.g. [1]) is used for integration of INS and GPS attitude because it in general is more accurate than the standard Kalman filter or the linearized Kalman filter. On the other hand, the EKF is an ad hoc algorithm with a higher risk of divergence than the standard Kalman filter, since the covariance equations are based on the linearized system and not the true nonlinear system. This also implies that optimality in the minimum variance sense cannot be guaranteed, although in many cases it will be very close. Local asymptotic stability of the EKF when used as an observer has been shown by [2], but there are no general conditions for guaranteeing *global* asymptotic stability of the EKF. The purpose of this paper is to give an alternative to the EKF for attitude integration purposes, and to evaluate both approaches.

The observer will be designed using nonlinear estimation theory, which basically means that the dynamic model and measurement updates of the observer are constructed such that stability is achieved in a Lyapunov sense given certain conditions on parameters and gains. In most cases, it is not straightforward to show Lyapunov stability. Background on nonlinear systems theory can be found in e.g. [3]. When designing the observer using this approach, robust stability is emphasized instead of (sub) optimality. Also, since no covariance matrix updates are required, the observer offers computational advantages.

2 MODELLING AND STABILITY

In this section, we will first present basic attitude theory. Then the observer is described and proven exponentially stable. Finally, the influence of noise and other errors on stability is investigated.

2.1 INS Attitude Modelling

We have chosen to represent attitude using quaternions. This is the most popular representation due to computational efficiency and absence of singularities. The set $\mathcal{H}$ of *unit quaternions* is defined as

$$\mathcal{H} = \left\{ \mathbf{q} \mid \mathbf{q}^T\mathbf{q} = 1, \mathbf{q} = [\boldsymbol{\eta},\ \boldsymbol{\varepsilon}^T]^T, \boldsymbol{\eta} \in \Re, \boldsymbol{\varepsilon} \in \Re^3 \right\}$$

Attitude error can readily be described using the quaternion product, $\tilde{\mathbf{q}} = \mathbf{q}^* \otimes \mathbf{q} \in \mathcal{H}$, where the product $\otimes$ is defined as

$$\begin{aligned} \tilde{\mathbf{q}} &= \hat{\mathbf{q}}^* \otimes \mathbf{q} = \begin{pmatrix} \hat{\eta} \\ -\hat{\boldsymbol{\varepsilon}} \end{pmatrix} \otimes \begin{pmatrix} \eta \\ \boldsymbol{\varepsilon} \end{pmatrix} \\ &\triangleq \begin{bmatrix} \hat{\eta} & \hat{\boldsymbol{\varepsilon}}^T \\ -\hat{\boldsymbol{\varepsilon}} & \hat{\boldsymbol{\eta}} - \mathbf{S}(\hat{\boldsymbol{\varepsilon}}) \end{bmatrix} \begin{bmatrix} \eta \\ \boldsymbol{\varepsilon} \end{bmatrix} \end{aligned} \tag{1}$$

and $\hat{\mathbf{q}}^* = [\hat{\eta}, -\hat{\boldsymbol{\varepsilon}}]^T$. The negative vector part represent rotation in the opposite direction. Zero attitude error is represented by $\tilde{\mathbf{q}} = [\pm 1, 0, 0, 0]^T$. Notice that quaternions give double coverage of $SO(3)$, and that $\tilde{\eta} = \pm 1$ represent the same attitude error.

The dynamics associated with the *unit quaternions* takes the form:

$$\begin{aligned} \dot{\mathbf{q}} &= \frac{1}{2} \begin{bmatrix} -\boldsymbol{\varepsilon}^T \\ [\eta \mathbf{I} + \mathbf{S}(\boldsymbol{\varepsilon})] \end{bmatrix} \boldsymbol{\omega}_{ib}^b \\ &\quad -\frac{1}{2} \begin{bmatrix} -\boldsymbol{\varepsilon}^T \\ [\eta \mathbf{I} - \mathbf{S}(\boldsymbol{\varepsilon})] \end{bmatrix} \boldsymbol{\omega}_{il}^l \\ &= \Omega(\mathbf{q}) \boldsymbol{\omega}_{ib}^b - \Xi(\mathbf{q}) \boldsymbol{\omega}_{il}^l \end{aligned} \tag{2}$$

where $\boldsymbol{\omega}_{il}^l = \boldsymbol{\omega}_{ie}^l + \boldsymbol{\omega}_{el}^l$.is assumed known and

$$\Omega(\mathbf{q}) = \frac{1}{2} \begin{bmatrix} -\boldsymbol{\varepsilon}^T \\ [\eta \mathbf{I} + \mathbf{S}(\boldsymbol{\varepsilon})] \end{bmatrix}$$

and

$$\Xi(\mathbf{q}) = \frac{1}{2} \begin{bmatrix} -\boldsymbol{\varepsilon}^T \\ [\eta \mathbf{I} - \mathbf{S}(\boldsymbol{\varepsilon})] \end{bmatrix}$$

When bias, scale-factor and misalignment errors and noise are included, (2) is written:

$$\dot{\mathbf{q}} = \Omega(\mathbf{q}) \left[(\mathbf{I} + \Delta) \boldsymbol{\omega}_{\text{imu}} + \mathbf{b} + \mathbf{w}_1 \right] - \Xi(\mathbf{q}) \boldsymbol{\omega}_{il}^l \tag{3}$$

where

$$\Delta = \Delta(\boldsymbol{\kappa}, \boldsymbol{\alpha}) = \begin{bmatrix} \kappa_x & \alpha_{xy} & \alpha_{xz} \\ \alpha_{yx} & \kappa_y & \alpha_{yz} \\ \alpha_{zx} & \alpha_{zy} & \kappa_z \end{bmatrix}$$

is the matrix containing misalignments and scale factor errors, and $\mathbf{b}$ is the gyro drift.

The gyro error models are assumed to be described by the 1st-order models:

$$\begin{aligned} \dot{\mathbf{b}} &= -\mathbf{T}_1^{-1}\mathbf{b} + \mathbf{w}_2 \\ \dot{\boldsymbol{\kappa}} &= -\mathbf{T}_2^{-1}\boldsymbol{\kappa} + \mathbf{w}_3 \\ \dot{\boldsymbol{\alpha}} &= -\mathbf{T}_3^{-1}\boldsymbol{\alpha} + \mathbf{w}_4 \end{aligned} \tag{4}$$

driven by bounded signals $\mathbf{w}_i \in \Re^3$ $(i = 1, 2, 3, 4)$. The matrices $\mathbf{T}_i > 0$ $(i = 1, 2, 3)$ are diagonal matrices of time constants, $\boldsymbol{\kappa} = [\kappa_x, \kappa_y, \kappa_z]^T$ are three gyro scale factor errors, and $\boldsymbol{\alpha} = [\alpha_{xy}, \alpha_{xz}, \alpha_{yx}, \alpha_{yz}, \alpha_{zx}, \alpha_{zy}]^T$ are six small gyro misalignment angles. $\mathbf{b} = -\mathbf{b}_{\text{gyro}}$ represents the biases of the gyros.

2.2 GPS Attitude Measurement

The integration can be mechanized as a loosely coupled or tightly coupled system. In a loosely coupled system, the GPS measurements are given as quaternions. Several algorithms that compute quaternions from GPS differential phase measurements have been presented (See e.g. [4]). The measurements will be highly correlated due to the process of GPS attitude determination. The tightly (or closely) coupled configuration is more convenient for GPS error modelling, and the GPS differential phase measurements are obviously less correlated than the computed quaternion in the loosely coupled case. For tightly coupled integration, the update quaternion vector part $\tilde{\boldsymbol{\varepsilon}}$ can be approximated by:

$$\tilde{\boldsymbol{\varepsilon}} = \mathbf{H}^\dagger (\Delta\boldsymbol{\phi} - \Delta\hat{\boldsymbol{\phi}} + \boldsymbol{\nu}) \tag{5}$$

where $\boldsymbol{\nu}$ is a composite GPS error vector including multipath, line biases, and noise. $\Delta\boldsymbol{\phi}$ is the vector of differential phase measurements and $\mathbf{H}^\dagger$ is the pseudoinverse of

$$\mathbf{H} = \begin{bmatrix} 2\Lambda^T \mathbf{S}(\mathbf{a}_1) \\ \vdots \\ 2\Lambda^T \mathbf{S}(\mathbf{a}_m) \end{bmatrix}$$

where

$$\Lambda = \begin{bmatrix} \lambda_N^1 & \cdots & \lambda_N^n \\ \lambda_E^1 & \cdots & \lambda_E^n \\ \lambda_D^1 & \cdots & \lambda_D^n \end{bmatrix}$$

is the matrix of n Line of Sight (LOS) vectors given in the NED frame, and $\mathbf{a}_j$ is baseline j from a total of m baselines. $\Delta\hat{\boldsymbol{\phi}}$ is the vector of differential phase estimates, where each element is calculated from INS unit quaternion estimates

$$\Delta\hat{\boldsymbol{\phi}}_{ij} = \boldsymbol{\lambda}_i^T \mathbf{R}(\hat{\mathbf{q}}) \mathbf{a}_j$$

where $\mathbf{R}$ is the associated rotation matrix. In the following, we will assume that $\tilde{\boldsymbol{\varepsilon}}$, the unit error quaternion vector part, is available. The approximation (5) may not be accurate for large angle errors. In this case higher order terms may be added or one of the attitude determination algorithms found e.g. in [4], can be used at a higher rate to arrive at the correct error quaternion.

2.3 Attitude Observer

The nonlinear observer of Salcudean [5] is extended to

include bias and error update laws according to:

$$\begin{aligned}
\dot{\hat{\mathbf{q}}} &= \Omega(\hat{\mathbf{q}})\left[(\mathbf{I}+\hat{\Delta}_1)\boldsymbol{\omega}_{\text{imu}} + \hat{\mathbf{b}}_1 + \mathbf{K}_1\tilde{\boldsymbol{\varepsilon}}\,\text{sgn}(\tilde{\eta})\right] - \Xi(\hat{\mathbf{q}})\boldsymbol{\omega}_{il}^{l} \\
\dot{\hat{\mathbf{b}}} &= -\mathbf{T}_1^{-1}\hat{\mathbf{b}} + \mathbf{K}_2\tilde{\boldsymbol{\varepsilon}}\,\text{sgn}(\tilde{\eta}) \qquad (6)\\
\dot{\hat{\boldsymbol{\kappa}}} &= -\mathbf{T}_2^{-1}\hat{\boldsymbol{\kappa}} + \mathbf{K}_3\text{diag}(\tilde{\boldsymbol{\varepsilon}})\,\boldsymbol{\omega}_{\text{imu}}\,\text{sgn}(\tilde{\eta}) \\
\dot{\hat{\boldsymbol{\alpha}}} &= -\mathbf{T}_3^{-1}\hat{\boldsymbol{\alpha}} + \mathbf{K}_4\Gamma(\tilde{\boldsymbol{\varepsilon}})\,\boldsymbol{\omega}_{\text{imu}}\,\text{sgn}(\tilde{\eta})
\end{aligned}$$

where

$$\Gamma(\tilde{\boldsymbol{\varepsilon}}) = \begin{bmatrix} 0 & \tilde{\varepsilon}_1 & 0 \\ 0 & 0 & \tilde{\varepsilon}_1 \\ \tilde{\varepsilon}_2 & 0 & 0 \\ 0 & 0 & \tilde{\varepsilon}_2 \\ \tilde{\varepsilon}_3 & 0 & 0 \\ 0 & \tilde{\varepsilon}_3 & 0 \end{bmatrix}$$

The error model is found by combining (3), (4), and (6):

$$\begin{aligned}
\dot{\tilde{\mathbf{q}}} &= \Omega(\tilde{\mathbf{q}})\left[\tilde{\Delta}_1\boldsymbol{\omega}_{\text{imu}} + \tilde{\mathbf{b}}_1 - \mathbf{K}_1\tilde{\boldsymbol{\varepsilon}}\,\text{sgn}(\tilde{\eta})\right] \\
\dot{\tilde{\mathbf{b}}} &= -\mathbf{T}_1^{-1}\tilde{\mathbf{b}} - \mathbf{K}_2\tilde{\boldsymbol{\varepsilon}}\,\text{sgn}(\tilde{\eta}) \qquad (7)\\
\dot{\tilde{\boldsymbol{\kappa}}} &= -\mathbf{T}_2^{-1}\tilde{\boldsymbol{\kappa}} - \mathbf{K}_3\text{diag}(\tilde{\boldsymbol{\varepsilon}})\,\boldsymbol{\omega}_{\text{imu}}\,\text{sgn}(\tilde{\eta}) \\
\dot{\tilde{\boldsymbol{\alpha}}} &= -\mathbf{T}_3^{-1}\tilde{\boldsymbol{\alpha}} - \mathbf{K}_4\Gamma(\tilde{\boldsymbol{\varepsilon}})\,\boldsymbol{\omega}_{\text{imu}}\,\text{sgn}(\tilde{\eta})
\end{aligned}$$

Note that the equilibrium points $(\tilde{\eta}, \tilde{\boldsymbol{\varepsilon}}, \tilde{\mathbf{b}}_1, \tilde{\boldsymbol{\kappa}}, \tilde{\boldsymbol{\alpha}}) = (\pm 1, \mathbf{0}, \mathbf{0}, \mathbf{0}, \mathbf{0})$. The $\text{sgn}(\tilde{\eta})$ term ensures that both equilibrium points are stable. The observer will converge to the point that is closest to the state. That is, if $\tilde{\eta}$ at some point is negative, the observer will converge to $(-1, \mathbf{0}, \mathbf{0}, \mathbf{0}, \mathbf{0})$, which is the closer equilibrium. For the nominal stability analysis, assume first that $\boldsymbol{\nu} = \mathbf{0}$ and $\mathbf{w}_i = \mathbf{0}$, $(i = 1, 2, 3, 4)$. Then the following Theorem can be proved.

Theorem 1 (Exponentially Stable Attitude Observer) *The equilibrium points $(\pm 1, \mathbf{0}, \mathbf{0}, \mathbf{0}, \mathbf{0})$ of the error model (7) are exponentially stable if the gains $\mathbf{K}_i, (i = 1, 2, 3, 4)$ are chosen to be positive definite.*

Proof. Consider the following Lyapunov function candidate:

$$\begin{aligned}
V &= \frac{1}{2}\tilde{\mathbf{b}}^T\mathbf{K}_2^{-1}\tilde{\mathbf{b}} + \frac{1}{2}\tilde{\boldsymbol{\kappa}}^T\mathbf{K}_3^{-1}\tilde{\boldsymbol{\kappa}} + \frac{1}{2}\tilde{\boldsymbol{\alpha}}^T\mathbf{K}_4^{-1}\tilde{\boldsymbol{\alpha}} \\
&\quad + \begin{cases} (\tilde{\eta}-1)^2 + \tilde{\boldsymbol{\varepsilon}}^T\tilde{\boldsymbol{\varepsilon}} & \text{if } \tilde{\eta} \geq 0 \\ (\tilde{\eta}+1)^2 + \tilde{\boldsymbol{\varepsilon}}^T\tilde{\boldsymbol{\varepsilon}} & \text{if } \tilde{\eta} < 0 \end{cases}
\end{aligned}$$

The time derivative along the trajectory of (7) is:

$$\begin{aligned}
\dot{V} &= \tilde{\mathbf{b}}^T\mathbf{K}_2^{-1}\dot{\tilde{\mathbf{b}}} + \tilde{\boldsymbol{\kappa}}^T\mathbf{K}_3^{-1}\dot{\tilde{\boldsymbol{\kappa}}} + \tilde{\boldsymbol{\alpha}}^T\mathbf{K}_4^{-1}\dot{\tilde{\boldsymbol{\alpha}}} + \begin{cases} -\dot{\tilde{\eta}} & \text{if } \tilde{\eta} \geq 0 \\ \dot{\tilde{\eta}} & \text{if } \tilde{\eta} < 0 \end{cases} \\
&= -\tilde{\mathbf{b}}^T\mathbf{K}_2^{-1}\mathbf{T}_1^{-1}\tilde{\mathbf{b}} - \tilde{\mathbf{b}}^T\tilde{\boldsymbol{\varepsilon}}\,\text{sgn}(\tilde{\eta}) \\
&\quad - \tilde{\boldsymbol{\kappa}}^T\mathbf{K}_3^{-1}\mathbf{T}_2^{-1}\tilde{\boldsymbol{\kappa}} - \tilde{\boldsymbol{\kappa}}^T\text{diag}(\tilde{\boldsymbol{\varepsilon}})\,\boldsymbol{\omega}_{\text{imu}}\,\text{sgn}(\tilde{\eta}) \\
&\quad - \tilde{\boldsymbol{\alpha}}^T\mathbf{K}_4^{-1}\mathbf{T}_3^{-1}\tilde{\boldsymbol{\alpha}} - \tilde{\boldsymbol{\alpha}}^T\Gamma(\tilde{\boldsymbol{\varepsilon}})\,\boldsymbol{\omega}_{\text{imu}}\,\text{sgn}(\tilde{\eta}) \\
&\quad + \tilde{\boldsymbol{\varepsilon}}^T\left[\tilde{\Delta}_1\boldsymbol{\omega}_{\text{imu}} + \tilde{\mathbf{b}} - \mathbf{K}_1\tilde{\boldsymbol{\varepsilon}}\,\text{sgn}(\tilde{\eta})\right]\text{sgn}(\tilde{\eta}) \\
&= -\tilde{\mathbf{b}}^T\mathbf{K}_2^{-1}\mathbf{T}_1^{-1}\tilde{\mathbf{b}} - \tilde{\boldsymbol{\kappa}}^T\mathbf{K}_3^{-1}\mathbf{T}_2^{-1}\tilde{\boldsymbol{\kappa}} \\
&\quad - \tilde{\boldsymbol{\alpha}}^T\mathbf{K}_4^{-1}\mathbf{T}_3^{-1}\tilde{\boldsymbol{\alpha}} - \tilde{\boldsymbol{\varepsilon}}^T\mathbf{K}_1\tilde{\boldsymbol{\varepsilon}} \\
&< 0, \quad \forall\, \tilde{\mathbf{b}}, \tilde{\boldsymbol{\kappa}}, \tilde{\boldsymbol{\alpha}}, \tilde{\boldsymbol{\varepsilon}} \neq \mathbf{0}
\end{aligned}$$

where we have used:

$$\begin{aligned}
&\tilde{\eta}\dot{\tilde{\eta}} + \tilde{\boldsymbol{\varepsilon}}^T\dot{\tilde{\boldsymbol{\varepsilon}}} \equiv 0 \\
&\tilde{\boldsymbol{\varepsilon}}^T\tilde{\Delta}_1\boldsymbol{\omega}_{\text{imu}} = \tilde{\boldsymbol{\kappa}}^T\,\text{diag}(\tilde{\boldsymbol{\varepsilon}})\boldsymbol{\omega}_{\text{imu}} + \tilde{\boldsymbol{\alpha}}^T\Gamma(\tilde{\boldsymbol{\varepsilon}})\,\boldsymbol{\omega}_{\text{imu}}
\end{aligned}$$

From the relation $\tilde{\eta}^2 + \tilde{\boldsymbol{\varepsilon}}^T\tilde{\boldsymbol{\varepsilon}} \equiv 1$ it is seen that as $\tilde{\boldsymbol{\varepsilon}} \to \mathbf{0}$ exponentially, $|\tilde{\eta}| \to 1$ exponentially. This completes the proof. ■

The gains can in general be chosen diagonal. Due to the multiple equilibrium points, it can be discussed whether the observer, in strict mathematical terms, is globally convergent or not. But if we consider the rotation matrix associated with the quaternions, the rotation matrix error will converge to the identity matrix given any initial attitude error matrix. We will thus refer to the observer as *globally* stable.

2.4 Robust Stability

When noise and other errors are included, the error model (7) becomes

$$\begin{aligned}
\dot{\tilde{\mathbf{q}}} &= \Omega(\tilde{\mathbf{q}})\left[\tilde{\Delta}_1\boldsymbol{\omega}_{\text{imu}} + \tilde{\mathbf{b}} + \mathbf{w}_1 - \mathbf{K}_1(\tilde{\boldsymbol{\varepsilon}} + \mathbf{H}^{\dagger}\boldsymbol{\nu})\,\text{sgn}(\tilde{\eta})\right] \\
\dot{\tilde{\mathbf{b}}} &= -\mathbf{T}_1^{-1}\tilde{\mathbf{b}} - \mathbf{K}_2(\tilde{\boldsymbol{\varepsilon}} + \mathbf{H}^{\dagger}\boldsymbol{\nu})\,\text{sgn}(\tilde{\eta}) + \mathbf{w}_2 \\
\dot{\tilde{\boldsymbol{\kappa}}} &= -\mathbf{T}_2^{-1}\tilde{\boldsymbol{\kappa}} - \mathbf{K}_3\text{diag}(\tilde{\boldsymbol{\varepsilon}} + \mathbf{H}^{\dagger}\boldsymbol{\nu}) \qquad (8)\\
&\quad (\boldsymbol{\omega}_{\text{imu}} + \mathbf{w}_1)\,\text{sgn}(\tilde{\eta}) + \mathbf{w}_3 \\
\dot{\tilde{\boldsymbol{\alpha}}} &= -\mathbf{T}_3^{-1}\tilde{\boldsymbol{\alpha}} - \mathbf{K}_4\Gamma(\tilde{\boldsymbol{\varepsilon}} + \mathbf{H}^{\dagger}\boldsymbol{\nu}) \\
&\quad (\boldsymbol{\omega}_{\text{imu}} + \mathbf{w}_1)\,\text{sgn}(\tilde{\eta}) + \mathbf{w}_4
\end{aligned}$$

If we define the vector $\mathbf{x} = [\tilde{\mathbf{b}}, \tilde{\boldsymbol{\kappa}}, \tilde{\boldsymbol{\alpha}}, \tilde{\boldsymbol{\varepsilon}}]^T$, the matrices

$$\Upsilon(\cdot) = \begin{bmatrix} (\cdot)_b & (\cdot)_a & 0 & 0 & 0 & 0 \\ 0 & 0 & (\cdot)_c & (\cdot)_a & 0 & 0 \\ 0 & 0 & 0 & 0 & (\cdot)_b & (\cdot)_c \end{bmatrix}^T$$

$$\mathbf{Q} = \begin{bmatrix} \mathbf{K}_1 & 0 & \frac{1}{2}\text{diag}(\mathbf{w}_1) & \frac{1}{2}\Upsilon^T(\mathbf{w}_1) \\ 0 & \mathbf{K}_2^{-1}\mathbf{T}_1^{-1} & 0 & 0 \\ \frac{1}{2}\text{diag}(\mathbf{w}_1) & 0 & \mathbf{K}_3^{-1}\mathbf{T}_2^{-1} & 0 \\ \frac{1}{2}\Upsilon(\mathbf{w}_1) & 0 & 0 & \mathbf{K}_4^{-1}\mathbf{T}_3^{-1} \end{bmatrix}$$

and the vector

$$\mathbf{n} = \begin{bmatrix} \mathbf{w}_1 + \mathbf{K}_1\mathbf{H}^{\dagger}\boldsymbol{\nu} \\ \mathbf{K}_2^{-1}\mathbf{w}_2 + \mathbf{H}^{\dagger}\boldsymbol{\nu} \\ \mathbf{K}_3^{-1}\mathbf{w}_3 + \text{diag}(\omega_{\text{imu}} + \mathbf{w}_1)\mathbf{H}^{\dagger}\boldsymbol{\nu} \\ \mathbf{K}_4^{-1}\mathbf{w}_4 + \Upsilon(\omega_{\text{imu}} + \mathbf{w}_1)\mathbf{H}^{\dagger}\boldsymbol{\nu} \end{bmatrix}$$

the following collorary can be proven.

Corollary 2 (Ultimately bounded observer) *The solution $\mathbf{x}(t)$ of the error equations (7) is uniformly ultimately bounded with the bound $\|\mathbf{x}\| \leq \|\mathbf{Q}^{-1}\mathbf{n}\|$*

Proof. Following the outline of the proof of Theorem 1 above we get:

$$\dot{V} \leq -\mathbf{x}^T\mathbf{Q}\mathbf{x} + \mathbf{x}^T\mathbf{n}$$

	EKF	Observer
Roll bias	-0.0021 rad/s	-0.0022 rad/s
Pitch bias	0.0044 rad/s	0.0044 rad/s
Yaw bias	-0.00059 rad/s	-0.00053 rad/s

1. Gyro biases

Thus, when $\mathbf{K}_i, i \in [1,4]$ is chosen such that $\mathbf{Q}$ is positive definite, the solution $\mathbf{x}(t)$ will converge to the ball

$$\|\mathbf{x}\| \leq \|\mathbf{Q}^{-1}\mathbf{n}\|$$

■

3 EXPERIMENTAL DATA

The system was set up with three antennae on top of a 40 ft. boat in a triangular planar configuration. The baselines were about 2.5, 1,6 and ,1.6 meters respectively. The inertial measurements came from a Navia Maritime Motion Reference Unit (MRU 5), which employs Coriolis force based vibratory gyros. This is a medium cost unit used in many different marine applications. The system had no external references, making evaluation of accuracy difficult. But it was possible to get an impression whether the algorithms are performing at the same level. Figures 1–4 show the estimated roll, pitch and yaw angles and biases in roll, pitch and yaw rate. The biases, which is almost identical for the two algoritms, are shown in Table 1.

In addition, we tested performance when the inertial system was initialized with large errors. Roll, pitch and yaw were initialized to 45, 90 and 45 degrees respectively, which of course are not realistic values, but it is done to test the filters with extreme errors. The GPS attitude were about -67.6 degrees for yaw, 1.3 degrees for pitch and 0.8 degrees for roll. It was possible to make the EKF diverge, but only with the combination of large angles and large errors in covariance matrices. The figures does not show any differences except for the pitch angle, but the convergence time is about the same for the two algorithms.

4 CONCLUSIONS

A nonlinear observer for integration of INS and GPS have been designed and proven (globally) exponentially convergent. The observer is a robust alternative to the well known Extended Kalman filter for which only local stability can be guaranteed. Whether the system is tuned by determining covariance matrices or gains, adjustments through testing or simulations are usually necessary. The observer, with fewer parameters to adjust, offers an alternative to the rather cumbersome covariance tuning procedure, and also computational savings when propagating equations. The post processing runs of GPS and IMU data showed that the performance of the observer, both in steady state and with large initial errors, is as good as the performance of the EKF.

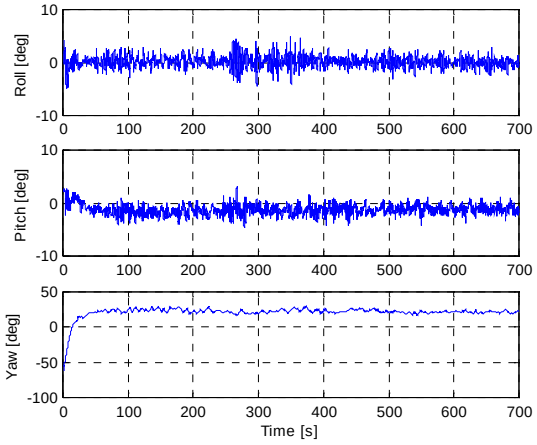

1. The figure shows the steady state performance of the EKF.

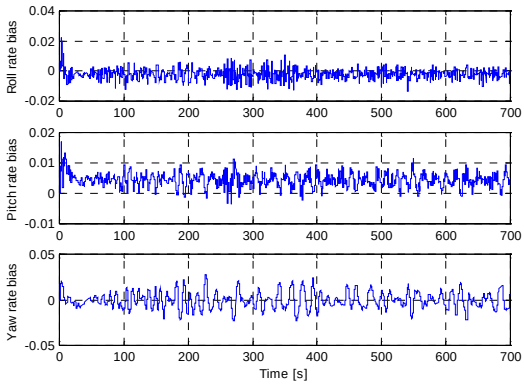

2. The figure shows bias estimation with the EKF.

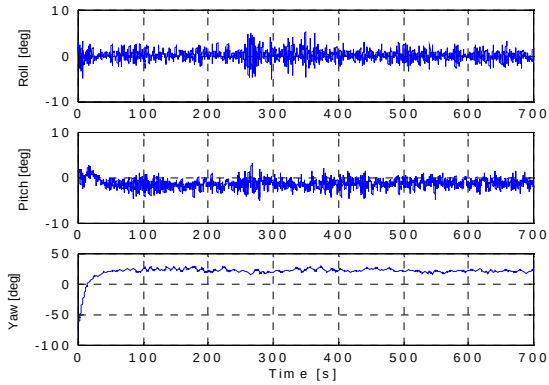

3. The figure shows the steady state performance of the observer.

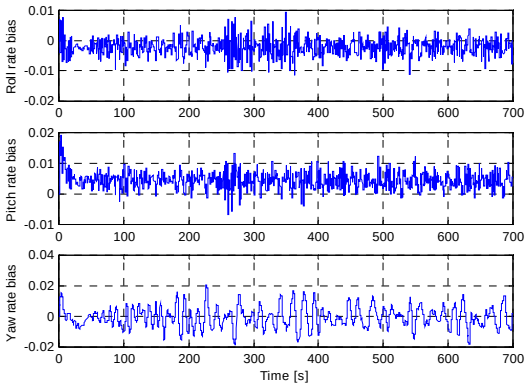

4. Bias estimation using the observer.

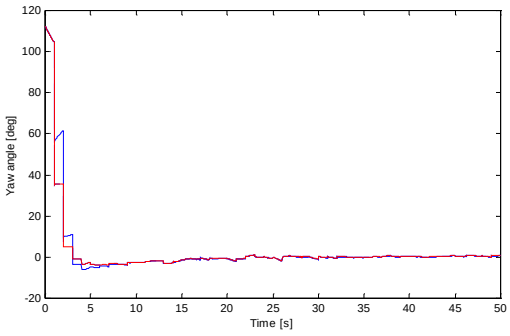

5. The yaw angle was initialized to 45 degrees, while the true initial yaw angle was -67.6 degrees. The observer error is in blue and the EKF error is in red.

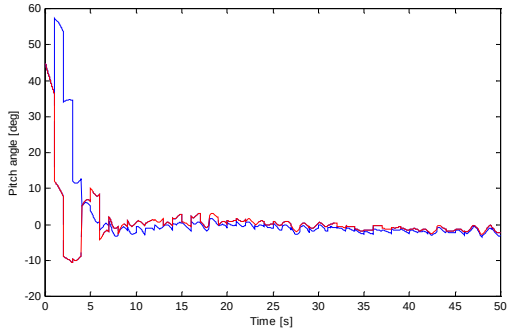

6. The initial pitch angle was 45 degrees, while the true angle was 1.3 degrees. The observer pitch error angle is in blue, and the EKF pitch error angle is in red.

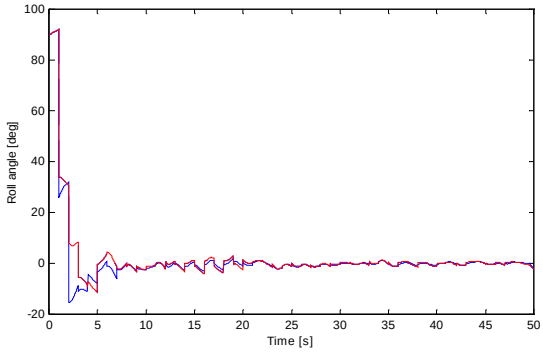

7. The initial roll angle was 90 degrees, while the true angle was 0.8 degrees. The observer roll error angle is in blue and the EKF roll error angle is in red.

ACKNOWLEDGMENTS

This work was sponsored by Navia Maritime, Division Seatex and the Norwegian Research Council. The authors are grateful to Navia Maritime, Division Seatex, and in particaular, Dr. John Morten Godhavn for providing experimental data.

REFERENCES

[1] A. Gelb, ed., *Applied Optimal Estimation*. Cambridge, MA: The MIT Press, 1974.

[2] M. Boutayeb, H. Rafaralahy, and M. Darouach, "Convergence Analysis of the Extended Kalman Filter Used as an Observer for Nonlinear Deterministic Discrete-Time Systems," *IEEE Trans. Automat. Contr.*, vol. 42, pp. 581–586, 1997.

[3] H. K. Khalil, *Nonlinear Systems*. Prentice Hall, Inc, 1996.

[4] I. Bar-Itzhack, P. Montgomery, and J. Garrick, "Algorithms for Attitude Determination Using GPS," in *Proceedings of the AIAA GNC Conf.*, (New Orleans, LA), 1997.

[5] S. Salcudean, "A Globally Convergent Angular Velocity Observer for Rigid Body Motion.," *IEEE Trans. Automat. Contr.*, vol. 36, pp. 1493–1497, 1991.